Energy Splitting of the Ground-State Doublet in the Nucleus ^{229}Th

B. R. Beck,[1] J. A. Becker,[1] P. Beiersdorfer,[1] G. V. Brown,[1] K. J. Moody,[1] J. B. Wilhelmy,[2] F. S. Porter,[3] C. A. Kilbourne,[3] and R. L. Kelley[3]

[1]*Lawrence Livermore National Laboratory, Livermore, California 94550, USA*
[2]*Los Alamos National Laboratory, Los Alamos, New Mexico 87545, USA*
[3]*NASA Goddard Space Flight Center, Greenbelt, Maryland 20771, USA*

(Received 24 October 2006; published 5 April 2007)

The energy splitting of the ^{229}Th ground-state doublet is measured to be 7.6 ± 0.5 eV, significantly greater than earlier measurements. Gamma rays produced following the alpha decay of ^{233}U (105 μCi) were counted in the NASA/electron beam ion trap x-ray microcalorimeter spectrometer with an experimental energy resolution of 26 eV (FWHM). A difference technique was applied to the gamma-ray decay of the 71.82 keV level that populates both members of the doublet. A positive correction amounting to 0.6 eV was made for the unobserved interband decay of the 29.19 keV state (29.19 $\rightarrow$ 0 keV).

DOI: 10.1103/PhysRevLett.98.142501 PACS numbers: 23.20.Lv, 27.90.+b

Nuclear level energies are generally much larger than atomic level energies, a fact that so far has precluded using atomic probes such as table-top lasers from exploiting atomic-nuclear couplings. The ground-state doublet of ^{229}Th is considered the premier candidate for bridging this coupling, as the first-excited state has energy $E(^{229m}\mathrm{Th})$ of a few eV—much lower than other nuclei—and the spin difference is 1 $\hbar$. The ability to manipulate a nuclear system "at will" with a laser offers a myriad of intriguing possibilities, including a clock with unparalleled precision for general relativity tests and measuring the variability of physical constants [1], a superb qubit for quantum computing, and tests of the effect of the chemical environment on nuclear decay rates [2]. These possibilities are enabled since compared to an atomic system a nucleus is exceptionally stable against external perturbations including collisions, because the characteristic nuclear dimension is much smaller than the atomic dimension and since the nucleus is shielded by the atomic electrons. Realizing these possibilities requires a precise measurement of $E(^{229m}\mathrm{Th})$. There are two ways to do so: (1) directly by observing the gamma ray given off in its decay and (2) indirectly using a differencing scheme involving gamma rays in decay paths of ^{229}Th states which include both the ground and first-excited states. A differencing scheme produced the currently accepted value of 3.5 ± 1.0 eV [3]. Subsequent direct measurements [4–7] have failed to detect this gamma ray. Here we employ a novel microcalorimeter to measure gamma rays produced in the alpha decay of ^{233}U, and we exploit a superior differencing scheme to obtain the energy splitting. We obtain $E(^{229m}\mathrm{Th}) = 7.6 \pm 0.5$ eV, twice the energy and more than 3 sigma removed from the previously accepted value—suggesting why prior direct observations have been unsuccessful.

An extremely low-lying state in the ^{229}Th nucleus was first proposed by Kroger and Reich [8]. They concluded that a $J^\pi = 3/2^+$ state lies within 0.1 keV of the $J^\pi = 5/2^+$ ground state based on their study of the ^{229}Th level structure with gamma-ray spectroscopy. Direct-reaction work [9] supported the inference of a doublet [8], as well as the Nilsson asymptotic quantum numbers $5/2^+[633]$ and $3/2^+[631]$ assigned by Ref. [8]. Reich and Helmer [10] developed more precise gamma-ray energy differences, and they deduced $E(^{229m}\mathrm{Th})$ as -1 ± 4 eV. Subsequently, Helmer and Reich [3] reported the splitting to be 3.5 ± 1.0 eV; see also Refs. [11–13]. Reanalyzing existing data, Guimarães-Filho and Helene [14] report $E(^{229m}\mathrm{Th}) = 5.5 \pm 1.0$ eV, but this value requires an unexpectedly large interband gamma-decay branching (25%) of the ^{229}Th 29.19 keV level to the ground state. The most accepted value remains 3.5 eV [3].

We took advantage of new detector technology to resolve the fortuitously closely spaced doublets following the

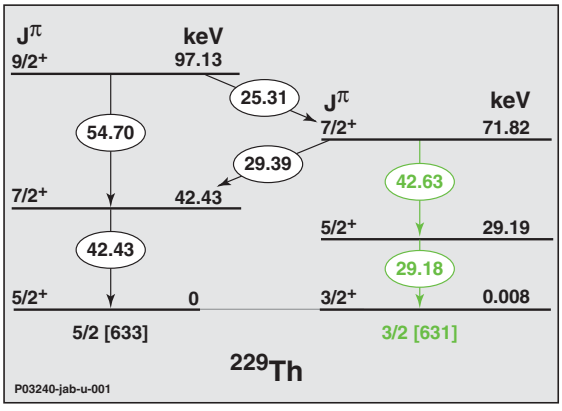

FIG. 1 (color). Partial level scheme of ^{229}Th with E_γ in keV. The two rotational bands are displaced relative to each other for clarity, and labeled by the Nilsson asymptotic quantum numbers. The gamma rays of the [631] band are distinguished by green coloring.

gamma-ray decay of the 71.82 keV state (see Fig. 1). The decay populates the first-excited state via inband transitions of 42.63 and 29.18 keV, as well as the ground state via an interband decay branch to the 42.43 keV state (E_γ = 29.39 keV) followed by a 42.43 keV transition. Therefore, $E(^{229m}\mathrm{Th})$ can be determined from the relationship $71.8\,\mathrm{keV} = 29.39 + 42.43\,\mathrm{keV} = 42.63 + 29.18\,\mathrm{keV} + E(^{229m}\mathrm{Th})$ or

$$E(^{229m}\mathrm{Th}) = \Delta E_{29} - \Delta E_{42}, \quad (1)$$

where $\Delta E_{29} = (29.39 - 29.18\,\mathrm{keV})$ and $\Delta E_{42} = (42.63 - 42.43\ \mathrm{keV})$.

The energy differences of each doublet are about 200 eV. Prior experiments employed Ge detectors for gamma-ray spectroscopy that cannot resolve the ΔE_{29} and ΔE_{42} doublets. These experiments relied on energy differences an order of magnitude or larger than 200 eV [3]. We employed the National Aeronautics and Space Administration (NASA) x-ray spectrometer (XRS) [15,16]. This microcalorimeter has sufficient energy resolution to resolve both ΔE_{29} and ΔE_{42}. The counting source can be placed within centimeters of the photon detectors eclipsing a relatively large solid angle, realizing a count rate commensurate with an experiment of a few weeks.

The XRS consists of 36 microcalorimeters (hereafter called pixels) in a 6×6 array of which 32 were electrically active in our experiment. Twenty-eight pixels used 8 μm thick HgTe absorbers and the remaining four used 30 μm thick Bi absorbers. The Bi absorbers had relatively poor energy resolution at the 90 mK operating temperature and they were not used in our analysis. Of the 28 HgTe pixels, 3 had excess noise in the electronics leaving 25 high-resolution pixels for spectroscopy. Each HgTe pixel is small—640 μm square. The detector system (similar to the XRS flight detector on the Suzaku Observatory [17]) is optimized to operate at 60 mK to provide maximum sensitivity with a relatively easy to obtain base temperature. Under these conditions, XRS had an approximately constant energy resolution of 6 eV (FWHM) and a 0.1–10 keV bandpass. To measure photon energies up to about 60 keV, we raised the operating temperature to 90 mK, which increases the dynamic range at the expense of energy resolution without requiring modification to the electronics system. At the 90 mK operating point, the resolution is ~26 eV (FWHM), roughly independent of photon energy.

We counted ^{229}Th gamma rays following ^{233}U alpha decay. The ^{233}U material was obtained in the following procedure. First, a sample of ^{232}Th was irradiated in a nuclear reactor. Second, the neutron capture product was chemically isolated as ^{233}Pa. Finally, the ^{233}Pa ($T_{1/2}$ = 27 d) decayed into ^{233}U—producing an isotopically pure sample. Using this technique, the ^{233}U is free of potentially interfering ^{232}U contaminants. (Some 69 photon lines between 40 and 500 keV—all of them attributed to the decay of ^{233}U—were identified in offline gamma-ray spectroscopy of the source.) The purified ^{233}U was electrodeposited onto 5 aluminum planchets, each 1.9 cm diameter and 254 μm thick. Total activity of the 5 planchets was 105 μCi. The planchets were mounted in an aluminum holder and covered with a 50.8 μm thick titanium foil. Maximum solid angle for counting was achieved by placing the ^{233}U source holder directly into the XRS detector module on the 1.5 K heat shield, 3.6 cm from the XRS detector array. In addition, an 865 μCi ^{241}Am calibration source was counted concurrently approximately 20% of the time. The ^{241}Am source was located inline with the XRS viewing port but outside of the XRS cryostat.

Counting lasted several weeks, and 11 good data sets (~24 h each) were obtained. The data acquisition system recorded the time, pixel, signal pulse height, signal rise time, a coincidence signal with a background particle detector placed directly behind the detector array, and a quality of signal for each photon event.

XRS events were converted to a pulse-height distribution (bins ~3 eV in the energy domain). The ΔE_{29} procedure was: (1) a small (<0.1%) slow drift in the XRS signal occurs during data collection. This drift was removed for each of the 11 data sets by applying a time-dependent scaling to each data set based on the time variation of the centroid of the strongest spectral peak (Th $L_{\beta 1}$). After scaling, the overall data set drift was significantly reduced, amounting to ~0.001%. (2) Next, for each pixel, each of the 11 data sets was scaled so the strongest spectral peak aligned across the 11 data sets (i.e., corrected for inter data set drift), and the 11 aligned spectra for each pixel were summed to produce a spectrum for that pixel that contained the signals from all 11 data sets. (3) The pixel summed pulse-height distribution was energy calibrated in the 0 to 33 keV range with the first 10 x rays and gamma rays listed in Table I, using a 4th order polynomial with zero-energy offset. (4) Finally, the energy calibrated and summed pixel spectra were added together to produce a single spectrum based on the 11 data sets and 25 pixels. Line shapes in the summed spectrum had a small (10%) increase in width compared to an individual pixel line shape.

The resultant summed spectrum near the 29 keV doublet is shown in Fig. 2(a). We find a raw ΔE_{29} of 205.58 ± 0.50 eV. We then fit 6 gamma-ray absorption peaks in the 26 to 33 keV energy region to a linear function to improve the energy calibration. The fitted peaks included two weak Am(59.5 keV) escape peaks which were not used in the original energy calibration, Am(59.5 keV) − Te $K_{\beta 1}$ and Am(59.5 keV) − Te $K_{\beta 3}$ (see Table I). The resulting slope was 0.999 527 ± 0.000 054, which we correct ΔE_{29} by and obtain ΔE_{29} = 205.48 ± 0.50 eV.

The 29.39 keV line has so few counts—about 2 per day per pixel—that summing all the data was necessary to produce a recognizable spectral feature. The ΔE_{42} procedure was similar to the ΔE_{29} procedure, but summing of all the data was not required as both spectral ΔE_{42} peaks had many more counts than the 29.39 keV peak (i.e., only steps 1–3 from above were performed). In addition, the energy

TABLE I. Calibration gamma- and x-ray energies, E, and uncertainties, σ.

ID	Calibration line	E (eV)	σ (eV)	Reference/Source
1	Ti $K_{\alpha 2}$ + Ti $K_{\alpha 1}$	4508.8[a]	0.04	[26]
2	Th $L_{\alpha 1}$	12 968.7	0.41	[26]
3	Th $L_{\beta 2}$ + Th $L_{\beta 4}$	15 630.5[b]	0.71	[26]
4	Th $L_{\beta 1}$	16 202.2	1.91	[26]
5	Th $L_{\beta 3}$	16 425.8	0.75	[26]
6	Th $L_{\gamma 1}$	18 982.5	0.87	[26]
7	Am(26.3 keV)	26 344.6	0.20	[27]
8	U(29.2 keV)	29 184.6	3.00	[3]
9	Am(59.5 keV) − Te $K_{\alpha 1}$	32 068.6	0.27	[26,27]
10	Am(59.5 keV) − Te $K_{\alpha 2}$	32 339.2	0.27	[26,27]
11	U(42.4 keV)	42 434.9[c]	2.4	
12	U(54.7 keV)	54 703.8	1.4	[3]
13	Am(59.5 keV)	59 540.9	0.20	[27]
14	Am(59.5 keV) − Te $K_{\beta 1}$	28 596.6	0.3	[26,27]
15	Am(59.5 keV) − Te $K_{\beta 3}$	28 596.6	0.3	[26,27]
16	Ti $K_{\alpha 2}$	4504.86	0.03	[26]
17	Ti $K_{\alpha 1}$	45 10.84	0.03	[26]
18	Hg $L_{\beta 1}$	11 822.6	0.6	[26]
19	Th $L_{\beta 4}$	15 425.8	0.6	[26]
20	Th $L_{\beta 2}$	15 623.7	0.6	[26]
21	Te $K_{\alpha 1}$	27 472.3	0.2	[26]
22	Te $K_{\alpha 2}$	27 210.7	0.2	[26]

[a]Calibration energy weighted by the fluorescent yields: $E(\text{cal}) = [E(\text{Ti}\,K_{\alpha 2}) + 2 \times E(\text{Ti}\,K_{\alpha 1})]/3$.

[b]Calibration energy weighted by the fluorescent yields: $E(\text{cal}) = [2 \times E(\text{Th}\,L_{\beta 2}) + E(\text{Th}\,L_{\beta 4})]/3$.

[c]$E(42\,434.9)$ eV was determined internally, measuring its Hg $L_{\beta 1}$ escape peak. Calibration was based on items 1–10 and 18 in this table.

calibration included three additional lines at higher energies (in total, the first 13 entries in Table I). The summed, energy-calibrated spectrum for a single pixel is shown in Fig. 2(b). For each data set, we applied the energy calibration to the 20 of 25 pixels which included the Am(59.5 keV) full-energy peak producing 220 spectra (11 data sets × 20 pixels). ΔE_{42} was obtained by fitting the two 42 keV peaks to determine the centroids, and subtracting for each of the 220 spectra. We calculate $\Delta E_{42} = 198.44 \pm 0.22$ eV.

We obtain from these measurements $\Delta E_{29} = 205.48 \pm 0.50$ eV and $\Delta E_{42} = 198.44 \pm 0.22$ eV, yielding $\Delta E_{29} - \Delta E_{42} = 7.0 \pm 0.5$ eV. The error is dominated by the centroid determination of the 29.39 keV gamma ray, weak in intensity since it is an interband transition between two rotational bands. Energy calibration errors are minimized because we only need to measure the small doublet energy differences accurately, not the absolute gamma-ray energies.

The measured difference of 7.0 ± 0.5 eV is not yet $E(^{229m}\text{Th})$, since a correction to ΔE_{29} is needed to account for the unobserved but expected interband branching of the 29.19 keV state to the ground state. The $(29.19 \rightarrow 0$ keV) branching can be estimated accurately from the interband branching ratio b of the 71.82 keV level, since the relevant nuclear structure for the two branching ratios is the same. The only difference in the branching ratios will be due to the difference in energy for the inband transitions out of the $7/2^+[631]$ level and out of the $5/2^+[631]$ level (42.63 and 29.19 keV, respectively). The M1 gamma ray transition rates scale as E_γ^3. We have measured the interband branching ratio, $b(71.82 \rightarrow 42.43\,\text{keV}; 7/2^+[631] \rightarrow 7/2^+[633]) = 1/37$ with an 8% error. Scaling gives the branching ratio $b(29.19 \rightarrow 0\,\text{keV}; 5/2^+[631] \rightarrow 5/2^+[633]) = 1/13$, with an 8% error, a value consistent with Ref. [3] who argue $b(29.19 \rightarrow 0\,\text{keV}) \sim 1/14$. It is also consistent with the width we measured for the 29.18 keV gamma-ray line shape, which suggests $b \leq 0.1$.

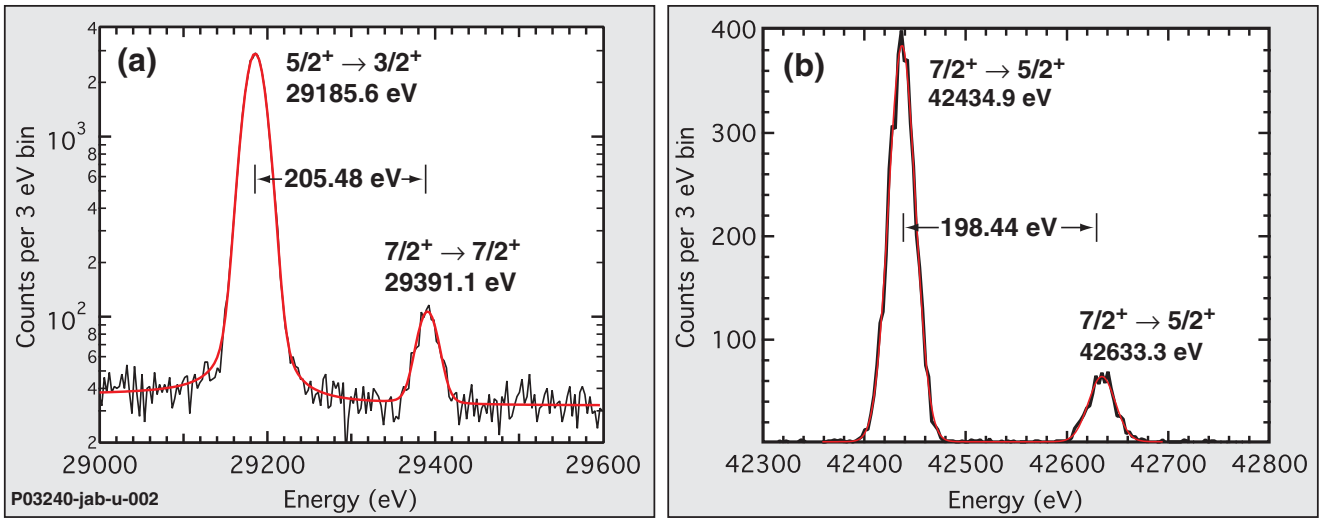

FIG. 2 (color). XRS spectra in the 29 and 42 keV energy regions. Data illustrated for the 29 keV doublet (ΔE_{29}) is the sum of 11 data sets and 25 pixels (a), and data illustrated for the 42 keV doublet (ΔE_{42}) represents the sum of 11 data sets only for pixel 0 (b). Black lines represent the data; red lines represent the least-square fitting results. Full-energy peaks are labeled by J^π of the corresponding ^{229}Th transition.

Using $b = 1/13$ the corrected $E(^{229m}\mathrm{Th}) = (\Delta E_{29} - \Delta E_{42})/(1 - b(29.19 \rightarrow 0\ \mathrm{keV})) = 7.6 \pm 0.5$ eV [18].

The lifetime of this state can be estimated from known experimental data. Helmer and Reich [3] pointed out that an M1 transition between the same two Nilsson states is observed in the deexcitation of the 312 keV level in ^{233}U, with transition strength $B(M1) = 0.0060\mu_N^2$ [19]. Scaling by E_γ^3 suggests a half-life of $\sim$5 h, consistent with the experimental report of Browne *et al.* [20]. Internal-conversion decay is energetically allowed, since the 7.6 eV level energy value is greater than the 6.3 eV ionization energy of an isolated thorium atom [21]. An estimate for the internal conversion lifetime for ^{229m}Th of $\sim$1000 h results from scaling the internal conversion of ^{235m}U. While the isomer lifetime is unlikely to be significantly altered by the opening of the internal-conversion branch because of the minimal phase space available for the outgoing electron, observation of the internal-conversion branch would be a delicate measurement of the energy of the isomer if the atomic environment was understood and controlled. Conversely the internal-conversion branch would afford an interesting probe of the atomic environment, since the branching is sensitive to both temperature and chemical environment. Finally, additional references discussing laser interactions with nuclei are given in Refs. [22–25].

Conversations with Zhen-Tian Lu, James Vary, Mort Weiss, A. K. Kerman, and Dennis McNabb are gratefully acknowledged. Thanks also to Andrea Kritcher and J. Ford Garberson who participated in early stages of this effort. The microcalorimeter spectrometer system XRS was developed by a large team at NASA/Goddard, particularly Christine Allen, Regis Brekosky, Kevin Boyce, John Gygax, and Jonathan King. This work was partially performed under the auspices of the U.S. Department of Energy by the Los Alamos National Security, LLC Los Alamos National Laboratory under Contract No. DE-AC52-06NA25396, and by the University of California, Lawrence Livermore National Laboratory under Contract No. W-7405-ENG-36. LLNL and NASA/GSFC also received support from NASA's Astronomy and Physics Research and Analysis Program under Purchase Request No. S-06563-G.

[1] E. Peik and Chr. Tamm, Europhys. Lett. **61**, 181 (2003).
[2] E. V. Tkalya, A. N. Zherikhin, and V. I. Zhudov, Phys. Rev. C **61**, 064308 (2000).
[3] R. G. Helmer and C. W. Reich, Phys. Rev. C **49**, 1845 (1994).
[4] G. M. Irwin and K. H. Kim, Phys. Rev. Lett. **79**, 990 (1997).
[5] D. S. Richardson, D. M. Benton, D. E. Evans, J. A. R. Griffith, and G. Tungate, Phys. Rev. Lett. **80**, 3206 (1998).
[6] S. B. Utter *et al.*, Phys. Rev. Lett. **82**, 505 (1999).
[7] R. W. Shaw, J. P. Young, S. P. Cooper, and O. F. Webb, Phys. Rev. Lett. **82**, 1109 (1999).
[8] L. A. Kroger and C. W. Reich, Nucl. Phys. **A259**, 29 (1976).
[9] D. G. Burke, P. E. Garrett, Tao Qu, and R. A. Naumann, Phys. Rev. C **42**, R499 (1990).
[10] C. W. Reich and R. G. Helmer, Phys. Rev. Lett. **64**, 271 (1990).
[11] V. Barci *et al.*, Phys. Rev. C **68**, 034329 (2003).
[12] K. Gulda *et al.*, Nucl. Phys. **A703**, 45 (2002).
[13] E. Ruchowska *et al.*, Phys. Rev. C **73**, 044326 (2006).
[14] Z. O. Guimarães-Filho and O. Helene, Phys. Rev. C **71**, 044303 (2005).
[15] F. S. Porter *et al.*, Rev. Sci. Instrum. **75**, 3772 (2004).
[16] C. K. Stahle *et al.*, Nucl. Instrum. Methods Phys. Res., Sect. A **520**, 466 (2004).
[17] R. L. Kelley, Nucl. Instrum. Methods Phys. Res., Sect. A **559**, 341 (2006).
[18] As written, the ΔE_{29} piece of Eq. (1) requires the centroid of the intraband $5/2^+ \rightarrow 3/2^+[631]$ transition. However, the measured ΔE_{29} is complex, since the 29.1 keV spectral peak [see Fig. 2(a)] represents the branching weighted sum of the two $\sim$29.1 keV decay spectral lines, the intraband $5/2^+ \rightarrow 3/2^+[631]$ and interband $5/2^+[631] \rightarrow 5/2^+[633]$ transitions. This introduces a correction term to $E(^{229m}\mathrm{Th})$ of Eq. (1), amounting to $bE(^{229m}\mathrm{Th})$, as follows. The measured ΔE_{29} is $29.39\ \mathrm{keV} - [(1 - b)E(5/2^+ \rightarrow 3/2^+) + b(E(5/2^+ \rightarrow 5/2^+))]$. The interband energy can be written explicitly in terms of $E(^{229m}\mathrm{Th})$ and the intraband transition energy, $E(5/2^+ \rightarrow 5/2^+) = E(5/2^+ \rightarrow 3/2^+) + E(^{229m}\mathrm{Th})$. Substituting, and using the measured ΔE_{29}, Eq. (1) becomes $E(^{229m}\mathrm{Th}) = [\Delta E_{29} + bE(^{229m}\mathrm{Th}) - \Delta E_{42}]$, or $E(^{229m}\mathrm{Th}) = (\Delta E_{29} - \Delta E_{42})/(1 - b)$.
[19] B. Singh and J. K. Tuli, Nuclear Data Sheets **105**, 109 (2005).
[20] E. Browne *et al.*, Phys. Rev. C **64**, 014311 (2001).
[21] S. Köhler *et al.*, Spectrochim. Acta, Part B **52**, 717 (1997).
[22] S. Matinyan, Phys. Rep. **298**, 199 (1998).
[23] E. V. Tkalya, JETP Lett. **55**, 211 (1992).
[24] D. S. Gemmell, in *Nuclear Transitions Induced by Synchrotron X-rays*, AIP Conf. Proc. No. 652 (AIP, New York, 2003), p. 239.
[25] T. J. Bürvenich, J. Evers, and C. H. Keitel, Phys. Rev. Lett. **96**, 142501 (2006).
[26] J. A. Bearden, Rev. Mod. Phys. **39**, 78 (1967).
[27] R. L. Heath, R. G. Helmer, J. R. Davidson, and R. J. Gehrke, Gamma-Ray Spectrum Catalogue, Ge and Si Detector Spectra, http://www.inl.gov/gammaray/catalogs/pdf/gecat.pdf.